Indonesian Journal of Electrical Engineering and Computer Science
Vol. 16, No. 1, October 2019, pp. 243~258
ISSN: 2502-4752, DOI: 10.11591/ijeecs.v16.i1.pp243-258

Selection of compression test images using variance-based statistical method

Allaoui Chems El houda, Bassou Abdesselam, Benyahia Ismahane, Khelifi Mustapha
Department of Electrical Engineering, Tahri Mohammed University-Bechar, Algeria

Article Info

Article history:

Received Jan 10, 2019
Revised Feb 12, 2019
Accepted Mar 15, 2019

Keywords:

Discrete Wavelet Transform
Evaluation Parameters
Image compression
JPEG
JPEG2000
Selection Algorithm
SPHIT

ABSTRACT

In this research paper, we used a variance-based statistical method to select 20 test images, according to these latter types (natural, satellite and medical) among a sample of 300 images (100 natural, 100 satellite and 100 medical). The images selection has been done using parameters of image quality, namely PSNR, MSSIM and VIF, which were applied on three compression algorithms (DWT+SPIHT, JPEG, and JPEG2000).

Corresponding Author:

Allaoui Chems El houda,
Department of National Chung,
Tahri Mohammed University-Bechar, Algeria.
Email: chems66@hotmail.com

1. INTRODUCTION

JPEG (Joint Photographic Experts Group) standard has been invented in 1986 by ISO (International Standards Organization) group and CEI (Commission Electronic International) group. It was aimed at compressing fixed color images at grey-scale data in order to save them on numerical support. One of common problems related to JPEG are mosaic appearances when compression levels are higher. This pushed researchers to search for a new standard to compress images: JPEG2000, which uses updated knowledge in the field of wavelets technology. At the heart of JPEG standard, we have discrete wavelet transform (DWT), while JPEG2000 heart consists of a breaking down into wavelets to allow a hierarchical representation of images in order to structure data efficiently, especially linking spectral content to a spatial position of the picture signal [1].

Other image compression algorithms, based on DWT, have been proposed in letterature. For example, the binary encoding algorithm named Set Partitionning In Hierarchical Tree (SPIHT) [2] was associated to the DWT in order to generate the DWT+SPIHT compression algorithm; this compression method was inverstigated on fix and motion images, and produce a suitable image quality according to [3].

The diversity of these compression algoritms has pushed us to propose a set of test images that permits to validate the effiency of future algorithms of image compression. The proposed images set is obtained by proposing a selection algorimth based on variance-based statistical method applied on image quality evaluation parameters.

2. METHODS OF IMAGES COMPRESSION

2.1. JPEG Transform

JPEG is a sophisticated compression method with or without losses whether at grey-scales or in color image. Such a standard does not handle monochromatic compression. It works for continuous tone images as well. One of the advantages of JPEG standard is that it uses many parameters which enable users to adjust lost data (i.e. compression level). Here are the main JPEG coding steps:

a) Preparation
b) TCD (Transform in Discrete Cosine) on 8x8 units
c) Quantification
d) Zigzag reading
e) DC component direct coding (average of 8x8 unit)
f) Coding by range of AC component (RLE: Run Length Encoding)
g) Entropic coding of Huffman [4] type (variable length coding: VLC).

For very high compression coding, we prefer compressing with wavelets or fractals to avoid edge effect which takes place sometimes under the shape of color rings near the remaining clear outlines.

2.2. JPEG 2000 Transform

JPEG 2000 is by its very nature multi-resolution standard, this allows us to compress, resolution by resolution, without redundancy, and eases transmission or direct coding with the most suitable resolution to our display system.

Moreover, it is possible to arrange information in the code stream with an increasing quality. Figure 1 represents the unit schema of a JPEG2000 coder. As it appears, a typical algorithm of JPEG2000 coding is mainly divided into 5 modules: Color transform, discrete wavelets transform, quantification, entropy coding unit and rate allowance [5]

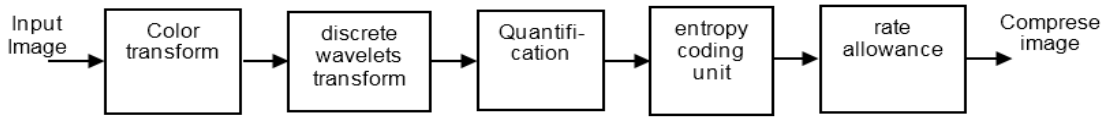

Figure 1. Typical Schema of a JPEG2000 Coder

2.3. Wavelet Transform

We can adapt wavelet transform in case of a discrete set. Such a technique is especially used with digital data with or without loss. Compression is achieved through successive approximations of initial information from the roughest to the finest. Therefore, we reduce information size by choosing a detail level [6].

Hence, we make a sampling of s and τ on a dyadic scale. We have then:

$$\psi_{m,n}[t] = s_0^{-m/2}\psi(s_0^{-m}t - n\tau_0) \quad (1)$$

Where s_0 and τ_0 are constants.

We define discrete wavelet transform as follows:

$$g[t] = \sum_{m\epsilon\mathbb{Z}}\sum_{m\epsilon\mathbb{Z}}\langle x, \psi_{m,n}\rangle . \psi_{m,n}[t] \quad (2)$$

2.3.1. Extending Wavelet Transform to Bi-dimensional Signals

Wavelet models can be generalized to every dimension n>0. In this research work, we make special emphasis on bi-dimensional cases to treat images [7-9].

Bi-dimensional signals are assumed measurable and having finite energy: $f(x,y) \in L^2(R^2)$.

Multi resolution analysis of $L^2(R^2)$ is obtained by defining it as a series of vector sub spaces V_j^2 of $L^2(R^2)$

We can define detail samples of j resolution as coefficients resulting from signal projection on W_j, orthogonal complement of V_j and V_{j-1}. We can define an orthonormal basis of W_j by translating and expanding three functions of 2D wavelet as follows:

$$\psi^1(x,y)=\phi(x)\psi(y)$$
$$\psi^2(x,y)=\psi(x)\phi(y)$$
$$\psi^3(x,y)=\psi(x)\psi(y)$$

These functions are verified, if $\psi^i_{j,k,l}(x,y)=2^{-j}\psi^i\left(2^{-j}x-k,2^{-j}y-l\right)$.

Hence $\left(\psi^1_{j,k,l},\psi^2_{j,k,l},\psi^3_{j,k,l}\right)_{(k,l)\in Z^2}$ is an orthonormal basis of W_j and $\left(\psi^1_{j,k,l},\psi^2_{j,k,l},\psi^3_{j,k,l}\right)_{(j,k,l)\in Z^3}$ and is an orthonormal basis of $L^2\left(R^2\right)$.

3. SPIHT CODING ALGORITHM (SET PARTITIONING IN HIERARCHICAL TREE)

SPIHT algorithm (Figure 2) (Set Partitioning In Hierarchical Tree), were suggested by Saïd and Pearlman. It is based on the following concepts: progressive coding by bit plans and using hierarchical dependencies which are sustained by coefficients of a 2D breaking down pyramid. SPIHT algorithm puts forward a list of insignificant sets (LSP), a list of insignificant coefficient (LIS) and a list of significant coefficient (LIP). This algorithm uses a description pass of insignificant coefficients and a refining pass [2, 3]

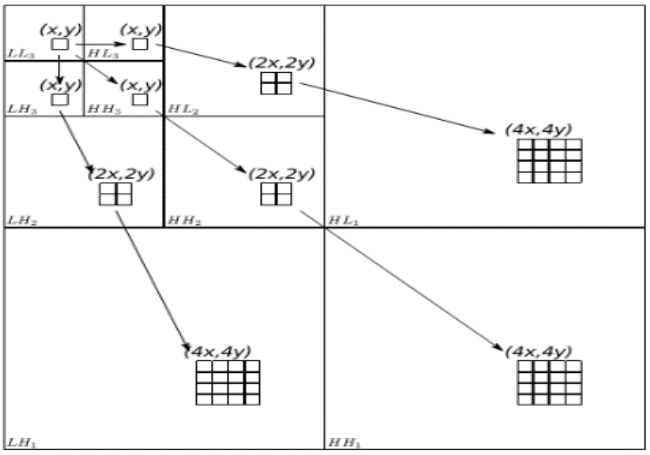

Figure 2. SPIHT Algorithm

4. QUALITY EVALUATION PARAMETERS

Measuring fidelity in compressing images is generally achieved by means of Mean Squaring Error MSE. Such a size (error) is defined by the mean square between the pixel (i,j) of the original image $I(i,j)$, and the pixel (i,j) of the reconstructed image $\hat{I}(i,j)$.

$$MSE=\frac{1}{M.N}.\sum_{m=0}^{M-1}\sum_{n=0}^{N-1}\left[I(i,j)-\hat{I}(i,j)\right]^2 \quad (3)$$

The peak signal to noise ratio [10]

$$PSNR=10.\log_{10}\frac{\left(2^R-1\right)^2}{MSE}\,[dB] \quad (4)$$

Afterwards, we evaluate a new paradigm to assess medical images quality. The similarity index compares brightness, contrast and structure between every vector pair, where structural similarity index (SSIM) between two signals x and y is expressed as follows: $SSIM(x,y)=l(x,y)c(x,y)s(x,y)$.

Finally, for the purpose, we need a single global measure of overall image quality that is given by the formula:

$$MSSIM\left(I,\hat{I}\right)=\frac{1}{M}\sum_{i=1}^{M}SSIM\left(I_i,\hat{I}_i\right) \quad (5)$$

M is the total number of local windows in the image. The values MSSIM exhibit greater consistency with the visual quality [11].

The Visual Information fidelity parameter (VIF) quantifies Shannon information that is shared between the reference and distorted images with respect to the information contained in the reference image itself [12].

VIF test is then evaluated as:

$$VIF = \frac{\sum_{j}^{M} I(C^{j}; \frac{F^{j}}{s^{j}})}{\sum_{j}^{M} I(C^{j}; \frac{E^{j}}{s^{j}})} \quad (6)$$

Where, I (X; Y/Z) is the conditional mutual information between X and Y, conditioned to Z; s^{j} is a realization of S^{j} for a particular image, the index j runs through all sub-bands in the decomposed image [13, 14].

5. RESULTS AND ANALYSIS

5.1. Method of Images Selection

In this research work, we have made choices, among 300 images (100 natural images, 100 satellite images and 100 medical images), according to the following criteria:

a. Histogram: It enables a great amount of information in terms of grey levels (intensity) distribution [15].
b. Entropy: It informs us about information quantity conveyed in the image [16].
c. Standard deviation: It is the intensity dispersion measurement regarding its average [15].

This research aim is to collect a set of 20 test images for every type (medical, satellite and natural), in order to check compression algorithms efficiency. We adopted a selection algorithm based on statistics achieved according to image evaluation parameters determined above.

5.2. Selection Algorithm for the Test Images

Selection algorithm for the test images is summarized in the flow chart of the Figure 3, It goes, after choosing N images (N=100 images in this paper) and K bit rates Rc for every image (in this paper, we took Rc=0.25,0.50,…,3.00, where K=12), through variances calculation [15] σ_(PSNR_i)^2, σ_(MSSIM_i)^2 et σ_(VIF_i)^2 evaluation parameters by

$$\sigma^{2}_{PSNR_i} = \frac{1}{K}\sum_{j=1}^{K}\left(PSNR_{i,j} - m_{PSNR_j}\right)^{2} \quad (7)$$

$$\sigma^{2}_{MSSIM_i} = \frac{1}{K}\sum_{j=1}^{K}\left(MSSIM_{i,j} - m_{MSSIM_j}\right)^{2} \quad (8)$$

$$\sigma^{2}_{VIF_i} = \frac{1}{K}\sum_{j=1}^{K}\left(VIF_{i,j} - m_{VIF_j}\right)^{2} \quad (9)$$

With, PSNR_(i,j), MSSIM_(i,j) and VIF_(i,j) are values of evaluation images parameters i=1…N and bit rates Rc_j, j=1…K. m_(PSNR_j), m_(MSSIM_j) et m_(VIF_j) are evaluation parameters averages for N images, and every Rc_j, calculated as follows:

$$m_{PSNR_j} = \frac{1}{N}\sum_{i=1}^{N} PSNR_{i,j} \quad (10)$$

$$m_{MSSIM_j} = \frac{1}{N}\sum_{i=1}^{N} MSSIM_{i,j} \quad (11)$$

$$m_{VIF_j} = \frac{1}{N}\sum_{i=1}^{N} VIF_{i,j} \quad (12)$$

The last step of the algorithm consists of selecting M images among N previous choices, based on variances thresholds choices S_{PSNR}, S_{MSSIM} et S_{VIF} enabling to save only the images $i = 1 \ldots N$ according to the following rules:

$\sigma^{2}_{PSNR_i} \leq S_{PSNR}$, $\sigma^{2}_{MSSIM_i} \leq S_{MSSIM}$ et $\sigma^{2}_{VIF_i} \leq S_{VIF}$

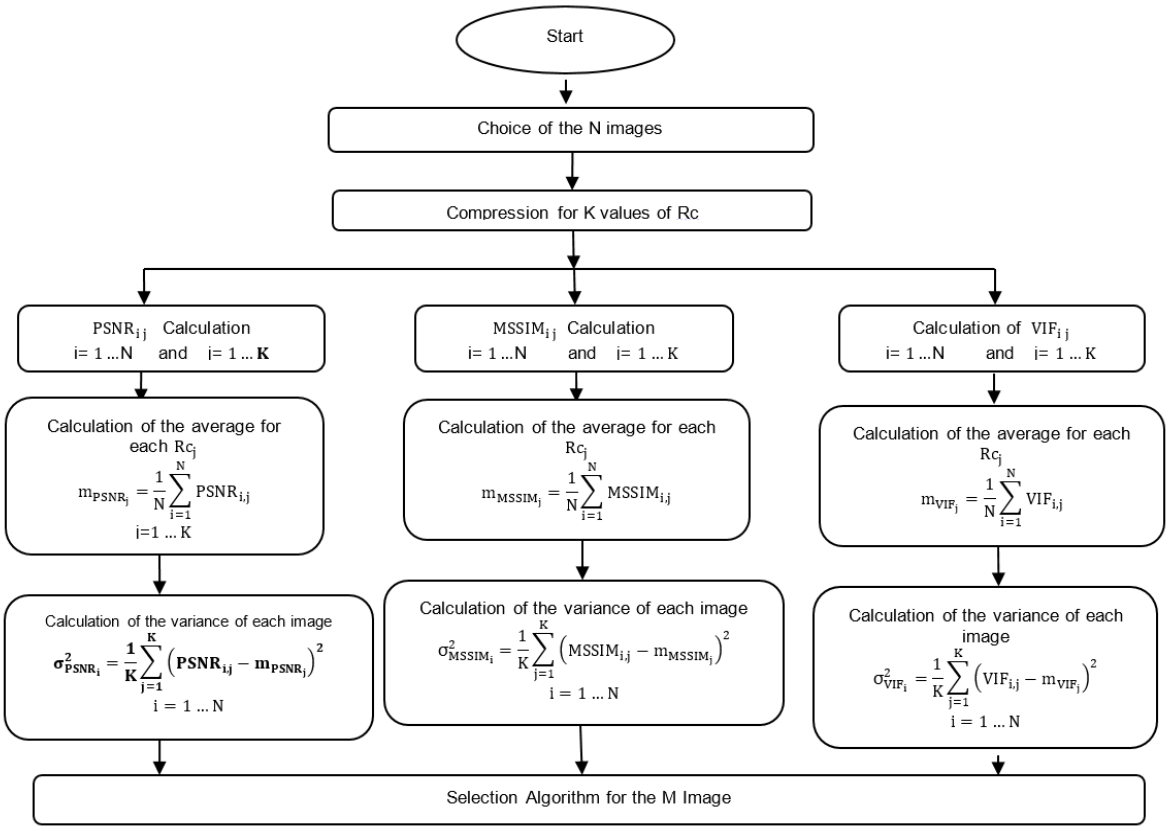

Figure 3. Chart of selection algorithm for test images

In order to give an example of the execution of the suggested algorithm, we chose $N = 5$ images (1, 9, 16, 31, 22) of size 512×512 in the grayscale (coded on 8bpp) represented in figure 4. We calculated three evaluation parameters PSNR, MSSIM, VIF in terms of bit rates $Rc = 0.25, 0.50, \ldots, 3.00$ ($K = 12$ Rc values), by adopting DWT/SPIHT as compression algorithm.

Boat (1) Clown (9) Lena (16) Bird (31) Woman (22)

Figure 4. Selected Images

Steps of averages calculation and variances of evaluation parameters are summarized in the Tables 1, 2 and 3. According to average variances column as it appears in the tables, the selection algorithm of test images accepts as values of variances thresholds

⟦0.2385<S⟧_PSNR<2.1170, 0.0000765<S_MSSIM<0.0002874 and ⟦0.0002507<S⟧_VIF<0.0003864 for M=1 image (in this case the test image is « 16 »). In the case where M=2, thresholds are as follows:

2.1170 <S_PSNR<3.8181, ⟦0.0002874 <S⟧_MSSIM<0.0003713 and 0.0003864 <S_VIF<0.0008309, and test images are « 16 » et « 9 ».

Table 1. PSNR Variation

Rc / image	0.25	0.50	0.75	1.00	1.25	1.50	1.75	2.00	2.25	2.50	2.75	3.00	
1	26.85	31.08	32.95	34.96	35.83	36.87	38.29	39.28	39.86	40.80	42.14	43.95	
9	27.83	31.86	34.14	36.60	38.01	40.20	41.23	42.29	43.75	45.09	45.92	46.55	
16	30.49	34.68	37.08	38.66	39.96	40.69	41.62	42.99	44.09	45.05	45.65	46.51	
31	31.81	37.39	39.82	41.95	43.09	44.54	45.42	46.07	47.02	48.16	49.72	50.77	Average Variance
22	31.84	36.36	38.59	40.64	41.70	42.72	44.26	45.26	45.84	46.75	47.94	49.63	
Average PSNR	29.76	34.27	36.52	38.56	39.72	41.01	42.17	43.18	44.11	45.1691	46.28	47.48	
1	08.48	10.21	12.72	13.02	15.14	17.12	15.03	15.21	18.08	19.11	17.08	12.49	14.47
9	03.73	05.81	05.66	03.84	02.92	00.65	00.87	00.78	00.13	00.01	00.13	00.87	02.12
16	00.52	00.17	00.32	00.01	00.06	00.10	00.30	00.04	00.00	00.01	00.39	00.95	00.24
31	04.18	09.69	10.93	11.50	11.36	12.53	10.61	08.38	08.47	08.92	11.86	10.81	09.94
22	04.31	04.35	04.31	04.32	03.94	02.95	04.40	04.33	02.99	02.51	02.77	04.63	03.82

Table 2. MSSIM Variation

Rc / image	0.25	0.50	0.75	1.00	1.25	1.50	1.75	2.00	2.25	2.50	2.75	3.00	
1	0.698	0.821	0.863	0.896	0.908	0.925	0.946	0.956	0.960	0.966	0.976	0.984	
9	0.746	0.880	0.925	0.949	0.960	0.973	0.976	0.980	0.985	0.988	0.990	0.991	
16	0.826	0.896	0.922	0.939	0.949	0.955	0.962	0.971	0.978	0.982	0.983	0.986	
31	0.871	0.932	0.951	0.963	0.969	0.977	0.980	0.982	0.985	0.989	0.992	0.994	Average Variance
22	0.851	0.918	0.939	0.955	0.960	0.967	0.976	0.980	0.982	0.985	0.988	0.992	
Average MSSIM	0.799	0.889	0.920	0.940	0.950	0.959	0.968	0.974	0.978	0.982	0.986	0.989	
1	0.0101	0.0047	0.0033	0.0019	0.0017	0.0012	0.0005	0.0003	0.0003	0.0002	0.0001	0.0000	0.0020
9	0.0028	0.0001	0.0000	0.0001	0.0001	0.0002	0.0001	0.0000	0.0001	0.0000	0.0000	0.0000	0.0003
16	0.0008	0.0001	0.0000	0.0000	0.0000	0.0000	0.0000	0.0000	0.0000	0.0000	0.0000	0.0000	0.0001
31	0.0053	0.0018	0.0010	0.0005	0.0004	0.0003	0.0001	0.0001	0.0001	0.0000	0.0000	0.0000	0.0008
22	0.0028	0.0008	0.0004	0.0002	0.0001	0.0001	0.0001	0.0000	0.0000	0.0000	0.0000	0.0000	0.0004

Table 3. VIF Variation

Rc / image	0.25	0.50	0.75	1.00	1.25	1.50	1.75	2.00	2.25	2.50	2.75	3.00	
1	0.265	0.424	0.501	0.569	0.604	0.641	0.689	0.722	0.740	0.771	0.810	0.853	
9	0.312	0.479	0.568	0.645	0.692	0.753	0.781	0.811	0.847	0.876	0.891	0.902	
16	0.386	0.540	0.614	0.664	0.706	0.731	0.763	0.805	0.835	0.859	0.871	0.891	
31	0.405	0.572	0.653	0.717	0.757	0.804	0.830	0.846	0.871	0.896	0.924	0.940	Average Variance
22	0.396	0.543	0.619	0.687	0.724	0.760	0.809	0.838	0.851	0.874	0.899	0.928	
Average VIF	0.353	0.512	0.591	0.656	0.697	0.738	0.774	0.804	0.829	0.855	0.879	0.903	
1	0.0076	0.0077	0.0082	0.0076	0.0086	0.0095	0.0073	0.0068	0.0079	0.0071	0.0048	0.0025	0.0071
9	0.0017	0.0010	0.0005	0.0001	0.0000	0.0002	0.0001	0.0000	0.0003	0.0004	0.0002	0.0000	0.0004
16	0.0011	0.0008	0.0005	0.0001	0.0001	0.0000	0.0001	0.0000	0.0000	0.0000	0.0001	0.0001	0.0003
31	0.0027	0.0036	0.0039	0.0037	0.0037	0.0043	0.0030	0.0018	0.0018	0.0017	0.0020	0.0014	0.0028
22	0.0019	0.0010	0.0008	0.0009	0.0007	0.0005	0.0012	0.0011	0.0005	0.0003	0.0004	0.0006	0.0008

To expand the application of the selection algorithm to M=20 images, we chose N=100 images (100 natural images, 100 satellite images and 100 medical images) of size 512×512 in the grayscale (coded on 8bpp). We adopted K=12 values of the bit rate Rc=0.25,0.50,…,3.00 and by using two wavelet-based compression algorithms and JPEG2000.

Selected images compressed by CDF9/7 algorithm with lifting structure and coupled with SPIHT encoder, gave the evaluation parameters (PSNR, MSSIM and VIF) values represented in Figures 5, 6, and 7. The variation intervals of the PSNR are as follows:

a. PSNR of 100 medical images varies between 25dB and 48dB for the bit rates Rc=0.25bpp , and between 45 dB and 68dB for the bit rates Rc=3bpp.
b. PSNR of 100 natural images varies between 20dB and 42dB for the bit rates Rc=0.25bpp , and between 35 dB and 62dB for the bit rates Rc=3bpp.
c. PSNR of 100 satellite images varies between 19 dB and 35dB for the bit rates Rc=0.25bpp , and between 32 dB and 52dB for the bit rates Rc=3bpp

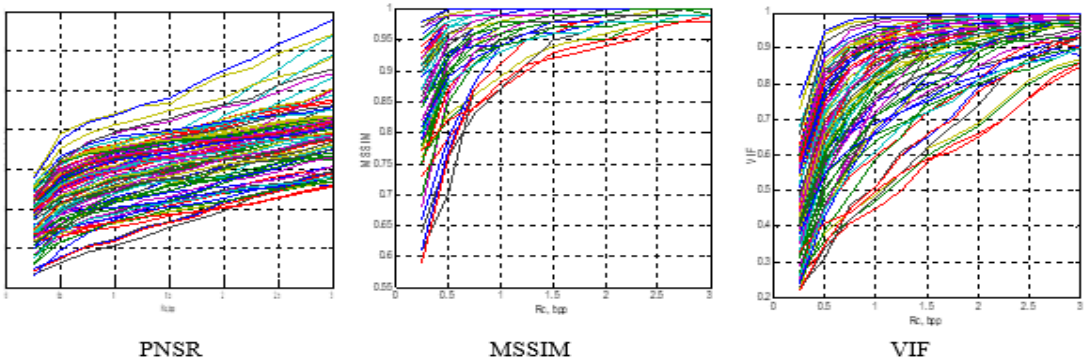

Figure 5. PSNR, MSSIM and VIF variation of 100 medical images

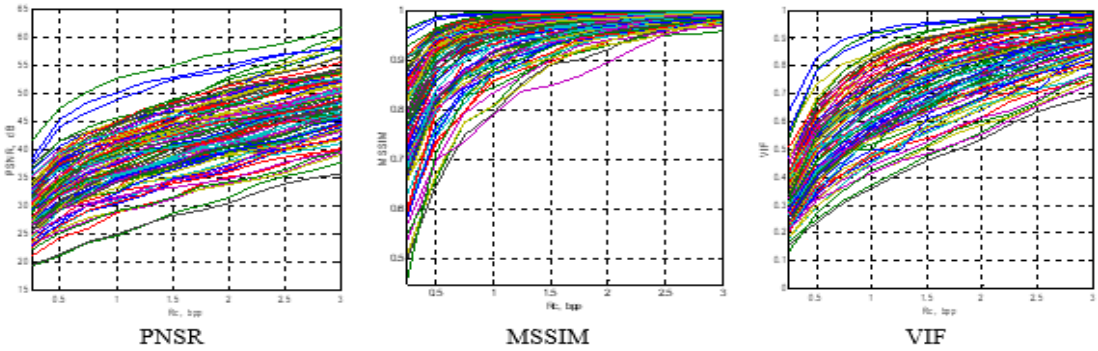

Figure 6. PSNR, MSSIM and VIF variation of 100 natural images

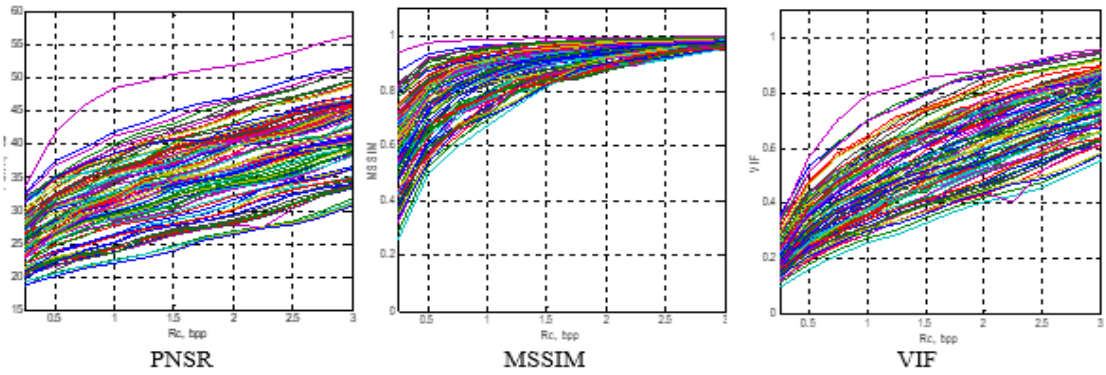

Figure 7. PSNR, MSSIM and VIF variation of 100 satellite images

Table 4 represents the resulting test Images by the selection algorithm, according to image types (medical, natural and satellite). In order to obtain the 20 test images, the applied thresholds on satellite images, enabled to choose 32 images from PSNR, 35 images from MSSIM and 38 images from VIF. For 20 natural test images, the selection algorithm selected 29 images from PSNR, 24 images from MSSIM and 42 images from VIF. The selected images for medicla images are, respectively, 21, 37 and 43. The test images are represented in Figures 8, 9, and 10.

Table 4. Resulting Test Images by the Selection Algorithm

Image Natural			Image Medical			Image Satellite		
PSNR	MSSIM	VIF	PSNR	MSSIM	VIF	PSNR	MSSIM	VIF
9	9	9	5	1	1	5	1	1
16	15	15	11	5	5	6	5	3
21	16	16	14	8	11	10	6	5
22	21	17	24	11	14	12	7	6
26	26	21	25	14	15	15	8	7
30	30	22	26	18	16	19	10	8
33	33	26	32	22	18	23	12	9
39	37	30	37	24	19	24	15	10
40	39	31	41	25	23	25	19	12
46	46	32	49	26	24	27	21	14
48	54	33	57	29	25	28	24	15
49	57	35	61	32	26	30	25	19
53	59	37	66	33	27	31	27	21
59	60	39	67	34	32	32	28	22
60	61	46	73	37	33	34	34	24
61	63	49	76	40	34	36	40	25
63	67	54	78	41	37	38	41	30
67	69	56	80	44	41	40	42	34
69	73	57	82	49	45	43	43	35
73	77	59	88	57	49	46	46	37
77	84	60	91	60	57	48	47	40
80	85	61		61	58	74	48	41
81	88	63		66	60	76	71	42
83	93	66		67	61	78	74	43
84		67		73	63	84	76	45
85		68		74	66	85	78	46
88		69		76	67	86	79	47
93		71		77	72	93	84	48
96		73		78	73	94	85	71
		74		80	74	95	86	74
		77		81	76	96	88	76
		80		82	77	97	93	78
		81		83	78		95	79
		83		84	80		96	85
		84		91	81		99	86
		85		96	82			93
		88		100	83			96
		93			84			99
		95			85			
		96			88			
		97			91			
		98			96			
					100			

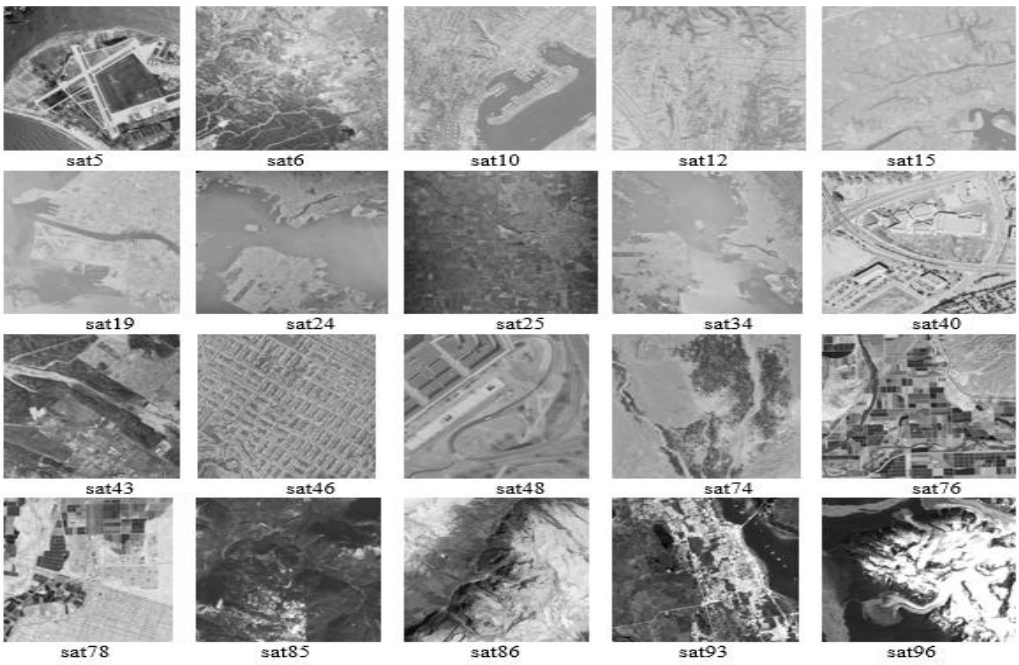

Figure 8. The 20 selected satellite test images

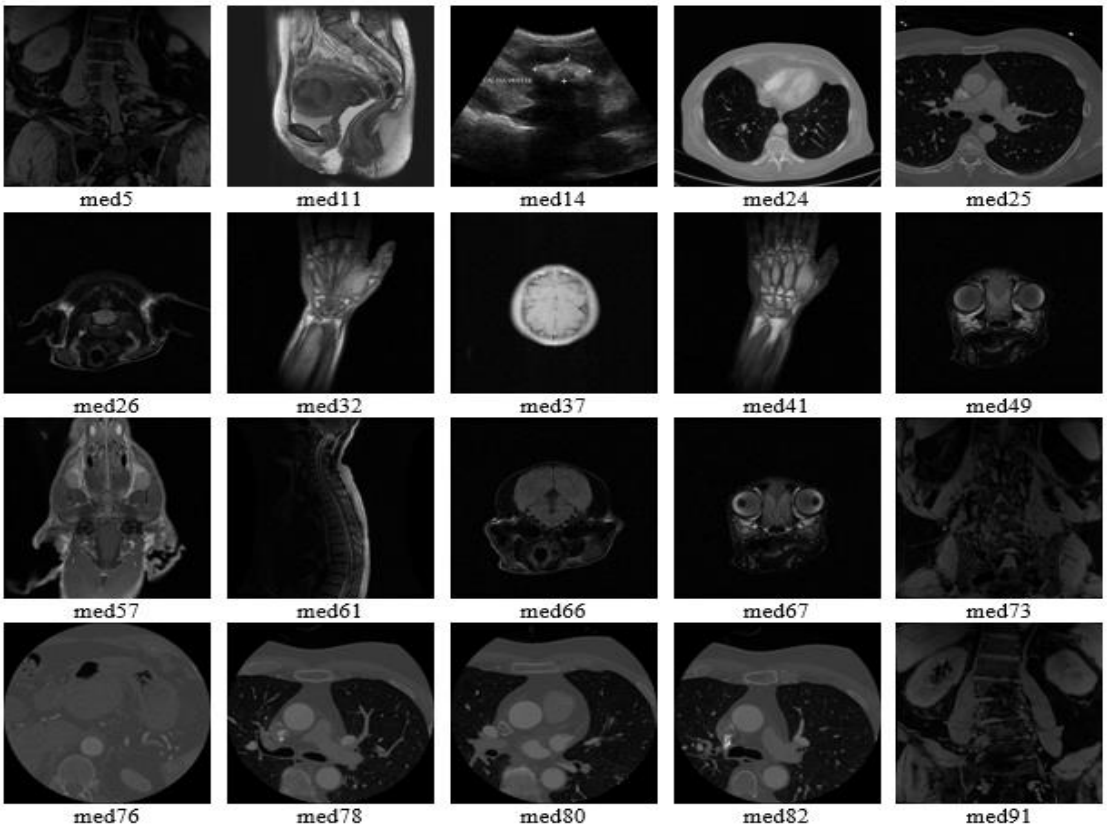

Figure 9. The 20 selected medical test images

Figure 10. The 20 selected natural test images

The evaluation parameters curves of the 20 test images per image type are represented in figures 11, 12 and 13. It can be observed that the loss in PSNR, MSSIM and VIF values is nearly constant whatever is the value of Rc for the three image types (medical, natural and satellite).

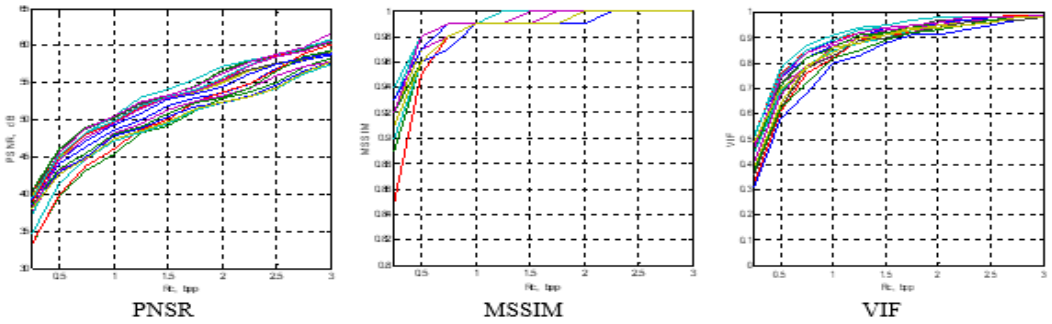

Figure 11. PSNR, MSSIM and VIF variations of the 20 selected medical test images using DWT+SPIHT

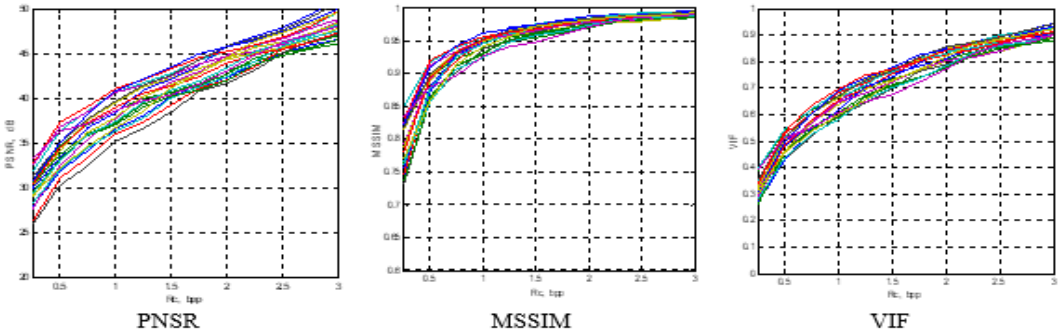

Figure 12. PSNR, MSSIM and VIF variations of the 20 selected natural test images using DWT+SPIHT

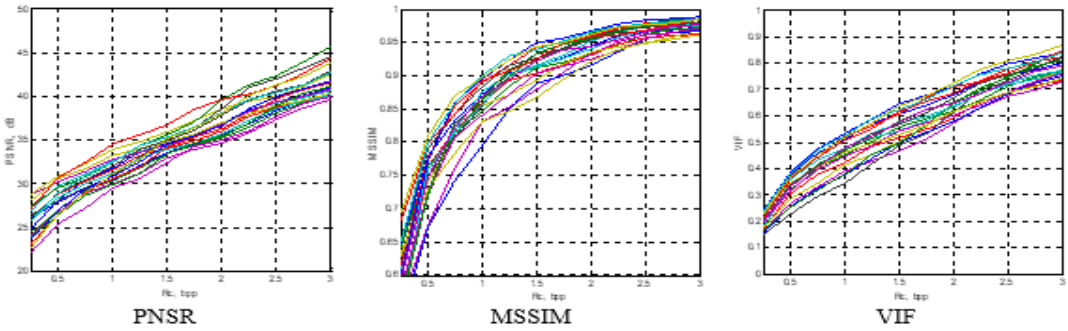

Figure 13. PSNR, MSSIM and VIF variations of the 20 selected satellite test images using DWT+SPIHT

The same prcedure was applied using JPEG 2000 standard as compression algorithm. The evaluation parameters variations are illustrated in Figures 14, 15 and 16. The variation intervals of the PSNR are as follows:

a. PSNR for 100 medical images varies between 26dB and 58dB for a bit rates of Rc=0.25bpp, and between 47dB and 60dB for a bit rates of Rc=3bpp.
b. PSNR for 100 natural images varies between 21dB and 47dB for a bit rates of Rc=0.25bpp, and between 39dB and 57dB for a bit rates of Rc=3bpp.
c. PSNR for 100 satellite images varies between 19dB and 40dB for a bit rates of Rc=0.25bpp, and between 33dB and 53dB for a bit rates of Rc=3bpp.

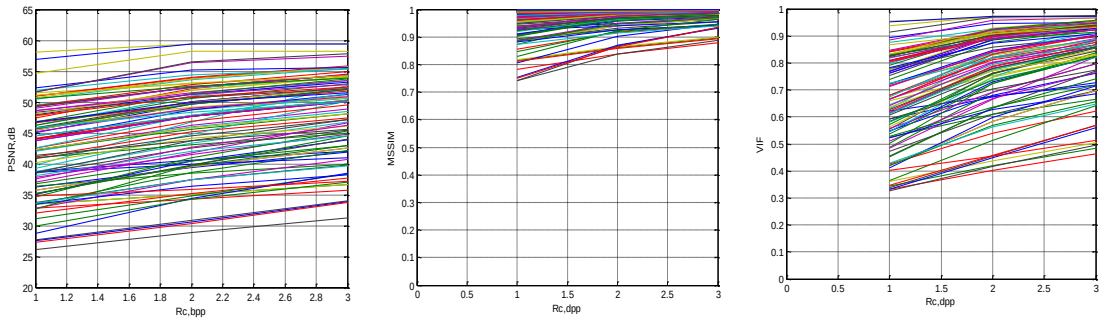

PSNR MSSIM VIF

Figure 14. The variations of PSNR, MSSIM and VIF of 100 medical images

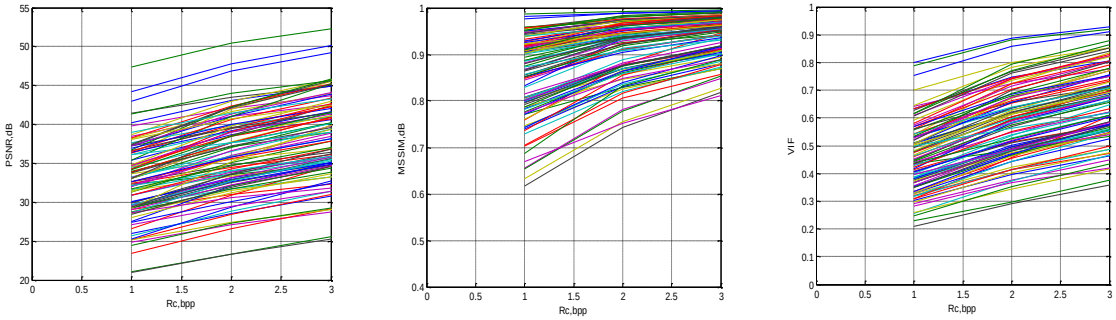

PSNR MSSIM VIF

Figure 15. The variations of PSNR, MSSIM and VIF of 100 natural images

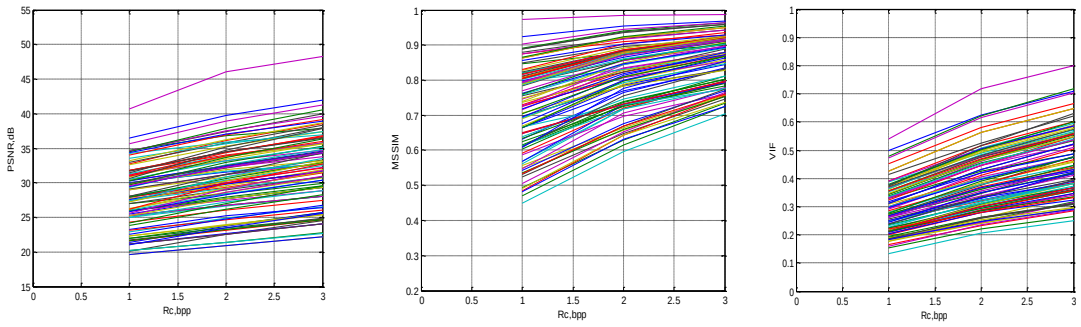

PSNR MSSIM VIF

Figure 16. The variations of PSNR, MSSIM and VIF of 100 satellite images

Table 5 represents the resulting test Images by the selection algorithm, according to image types (medical, natural and satellite). In order to obtain the 20 test images, the applied thresholds on satellite images, enabled to choose 28 images from PSNR, 28 images from MSSIM and 47 images from VIF. For 20 natural test images, the selection algorithm selected 37 images from PSNR, 35 images from MSSIM and 51 images from VIF.

The selected images for medical images are, respectively, 36, 35 and 34. The test images are represented in Figures 17, 18, and 19. It can be observed that the loss in PSNR, MSSIM and VIF values is nearly constant whatever is the value of Rc for the three image types (medical, natural and satellite).

Figures 20, 21, and 22 represent the curves of PSNR, MSSIM and VIF for the 20 selected images (obtained by combaning both DWT+SPIHT-based and JPEG 2000-based selection algorithms) according to image types (medical, natural and satellite) using JPEG standard. It can be observed that the loss in PSNR, MSSIM and VIF values is nearly constant whatever is the value of Rc for the three image types (medical, natural and satellite).

Table 5. PSNR, MSSIM and VIF thresholds

Image Natural			Image Medical			Image Satellite		
PSNR	MSSIM	VIF	PSNR	MSSIM	VIF	PSNR	MSSIM	VIF
5	1	1	5	1	1	5	1	1
11	5	5	11	5	5	6	5	3
14	8	11	14	8	11	10	6	5
24	11	14	24	11	14	12	7	6
25	14	15	25	14	15	15	8	7
26	15	24	26	15	24	19	10	8
29	23	25	29	23	25	21	12	9
32	24	26	32	24	26	24	15	10
34	25	32	34	25	32	25	18	12
36	26	33	36	26	33	27	19	14
37	32	34	37	32	34	28	21	15
41	33	37	41	33	37	31	22	18
42	35	41	42	35	41	32	24	19
44	37	45	44	37	45	34	25	21
45	40	49	45	40	49	36	27	22
47	41	61	47	41	61	38	28	23
48	44	63	48	44	63	40	34	24
49	49	66	49	49	66	43	37	25
57	60	67	57	60	67	46	40	27
58	66	72	58	66	72	48	41	28
61	67	73	61	67	73	74	42	30
66	72	74	66	72	74	76	43	31
67	73	76	67	73	76	78	45	32
73	74	77	73	74	77	85	46	34
76	76	78	76	76	78	86	47	35
77	77	80	77	77	80	93	48	36
78	78	81	78	78	81	95	60	37
80	80	82	80	80	82	96	70	38
81	81	83	81	81	83		71	39
82	82	84	82	82	84		72	40
83	83	88	83	83	88		73	41
84	84	91	84	84	91		74	42
85	91	96	85	91	96		76	43
88	96	100	88	96	100		78	45
91	100		91	100			79	46
96			96				81	47
							83	48
							84	71
							85	74
							86	76
							88	77
							89	78
							93	79
							95	84
							96	85
							97	86
							99	93
							95	95
							96	96
							99	99

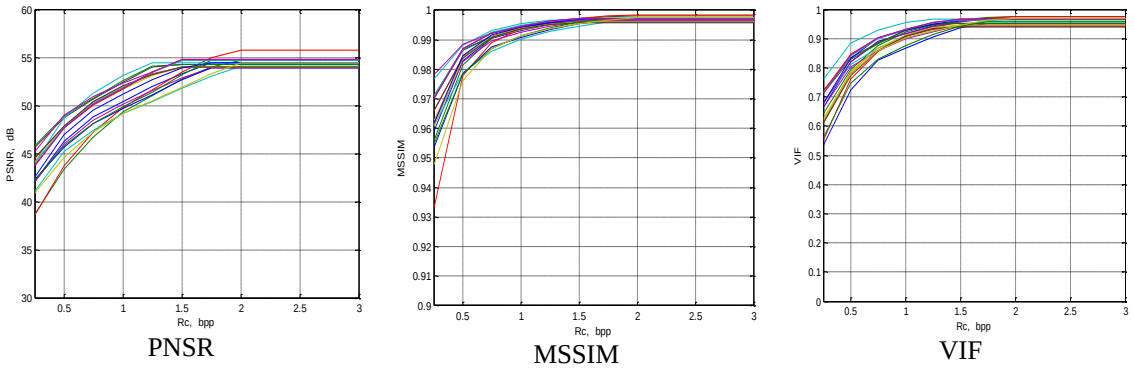

PNSR MSSIM VIF

Figure 17. PSNR, MSSIM and VIF variations of 20 selected medical test images using JPEG 2000 standard

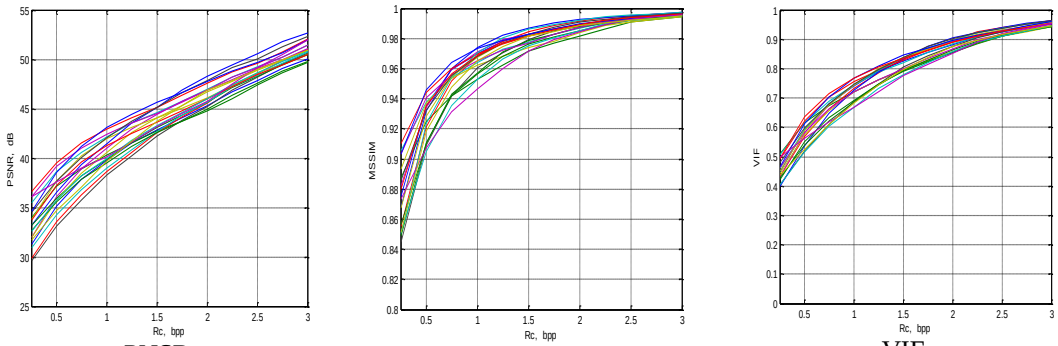

PNSR MSSIM VIF

Figure 18. PSNR, MSSIM and VIF variations of 20 selected natural test images using JPEG 2000 standard

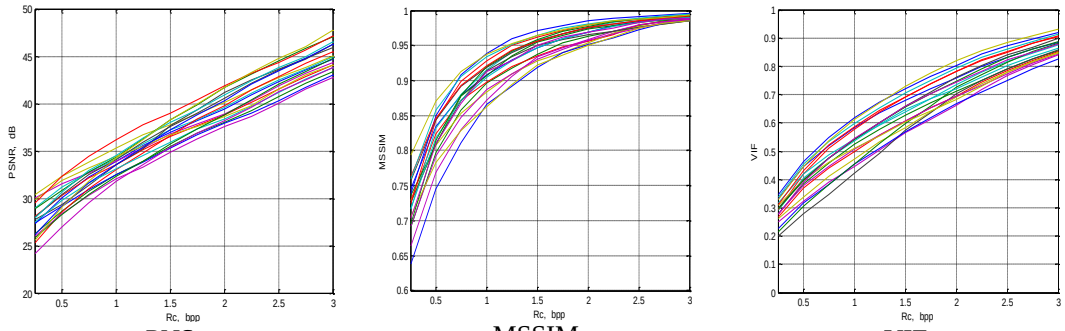

PNS MSSIM VIF

Figure 19. PSNR, MSSIM and VIF variations of 20 selected satellite test images using JPEG 2000 standard

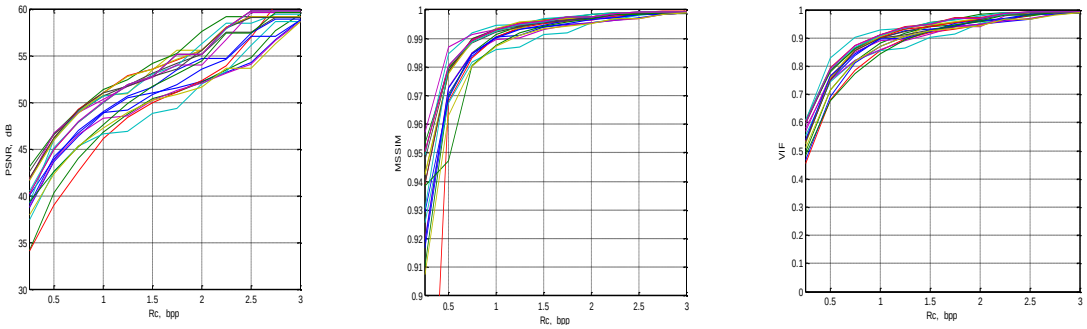

PNSR MSSIM VIF

Figure 20. PSNR, MSSIM and VIF variations of 20 selected medical test images using JPEG standard

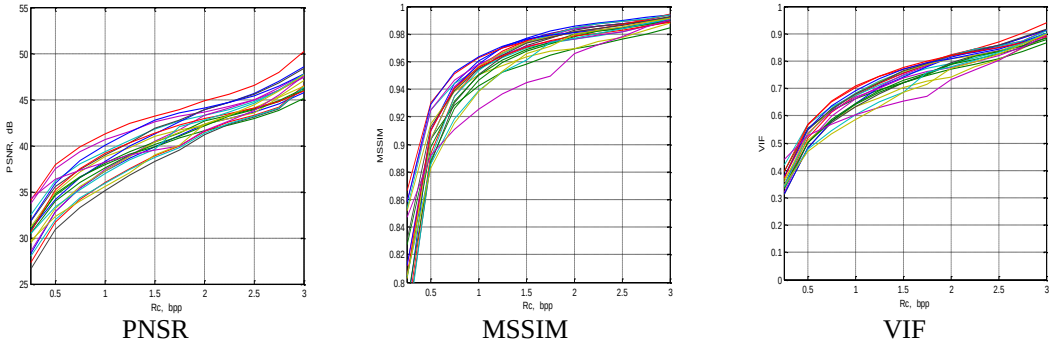

PNSR MSSIM VIF

Figure 21. PSNR, MSSIM and VIF variations of 20 selected natural test images using JPEG standard

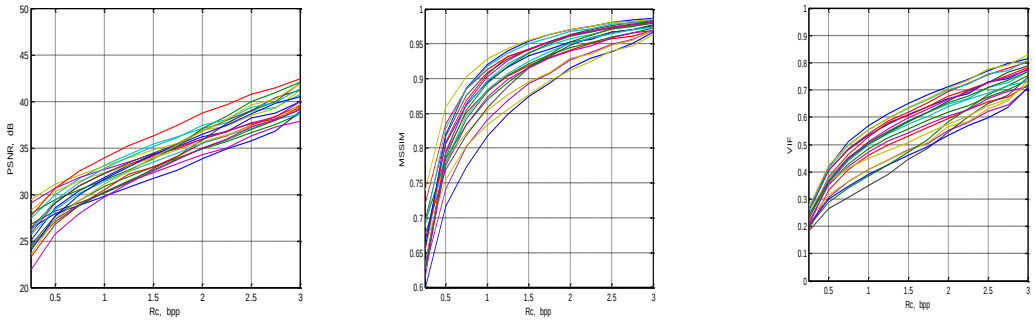

PNSR MSSIM VIF

Figure 22. PSNR, MSSIM and VIF variations of 20 selected satellite test images using JPEG standard

Table 6 shows the PSNR, MSSIM, and VIF variance of the 20 images selected for each type (medical, natural, and satellite) after applying the algorithm used.

Table 6. The variances of PSNR, MSSIM, and VIF for the 20 selected images per iamge type

Satellite image				Natural image				Medical image			
Image	$\sigma^2_{PSNR_i}$	$\sigma^2_{MSSIM_i}$	$\sigma^2_{VIF_i}$	Image	$\sigma^2_{PSNR_i}$	$\sigma^2_{MSSIM_i}$	$\sigma^2_{VIF_i}$	Image	$\sigma^2_{PSNR_i}$	$\sigma^2_{MSSIM_i}$	$\sigma^2_{VIF_i}$
5	0.22	0.0003	0.0023	9	2.11	0.0001	0.0001	5	0.81	0.0003	0.0020
6	2.15	0.0002	0.0001	16	1.35	0.0004	0.0007	11	5.39	0.0001	0.0007
10	0.64	0.0001	0.0012	21	3.46	0.0001	0.0004	14	2.93	0.0002	0.0022
12	0.57	0.0005	0.0002	26	0.59	0.0002	0.0007	24	4.30	0.0001	0.0004
15	1.32	0.0011	0.0040	30	1.11	0.0003	0.0002	25	1.23	0.0002	0.0011
19	2.88	0.0002	0.0014	33	5.91	0.0001	0.0014	26	2.42	0.0002	0.0009
24	2.80	0.0002	0.0045	39	2.20	0.0002	0.0014	32	4.80	0.0003	0.0014
25	1.27	0.0018	0.0032	46	0.78	0.0000	0.0008	37	2.68	0.0001	0.0032
34	4.89	0.0003	0.0027	59	1.46	0.0001	0.0008	41	5.35	0.0004	0.0012
40	1.40	0.0007	0.0024	60	3.72	0.0000	0.0002	49	3.03	0.0003	0.0013
43	0.83	0.0000	0.0005	61	0.18	0.0002	0.0008	57	5.01	0.0004	0.0047
46	3.81	0.0002	0.0005	63	5.82	0.0001	0.0034	61	4.54	0.0004	0.0005
48	1.58	0.0006	0.0008	67	3.12	0.0004	0.0011	66	2.55	0.0002	0.0011
74	0.53	0.0007	0.0007	69	4.08	0.0002	0.0011	67	3.05	0.0003	0.0013
76	0.80	0.0009	0.0053	73	1.75	0.0001	0.0010	73	1.39	0.0003	0.0028
78	2.14	0.0005	0.0004	77	2.90	0.0003	0.0023	76	0.68	0.0002	0.0009
85	5.06	0.0011	0.0030	84	0.86	0.0002	0.0013	78	2.46	0.0004	0.0032
86	0.73	0.0012	0.0043	85	0.11	0.0002	0.0014	80	3.06	0.0004	0.0032
93	5.72	0.0001	0.0002	88	2.41	0.0004	0.0014	82	1.84	0.0003	0.0023
96	2.58	0.0018	0.0054	93	0.96	0.0001	0.0007	91	3.10	0.0001	0.0006

To better evaluate the effectiveness of the selection algorithm, we traced on Figures 23, 24, and 25 the curves of the variance of each evaluation parameter for all types of images. It can be seen that a slight difference between the three compression algorithms; which makes it possible to say that the selected images are adequate for testing other image compression algorithms based on a transformation.

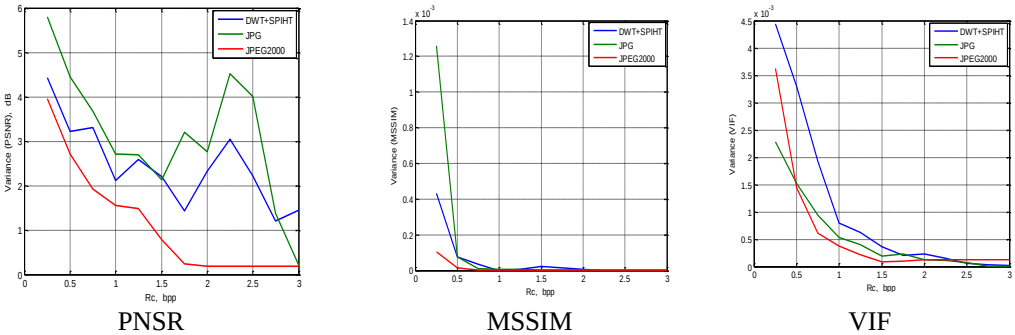

PNSR MSSIM VIF

Figure 23. The variation of the variance of PSNR, MSSIM and VIF for the 20 selected medical test images

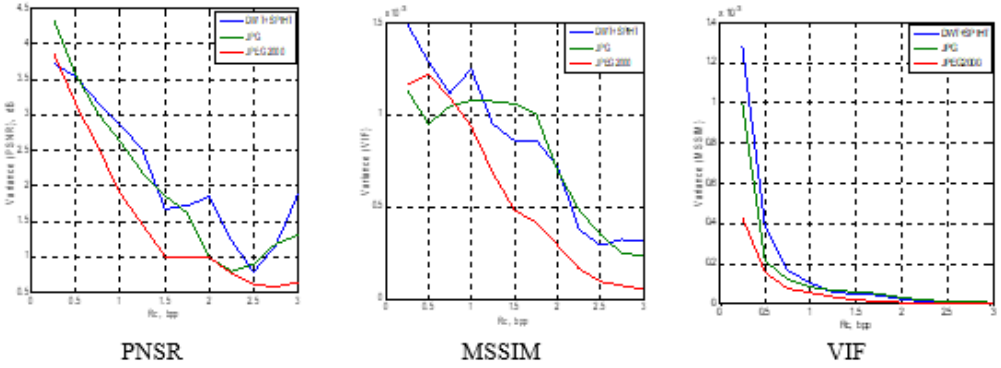

Figure 24. The variation of the variance of PSNR, MSSIM and VIF for the 20 selected natural test images

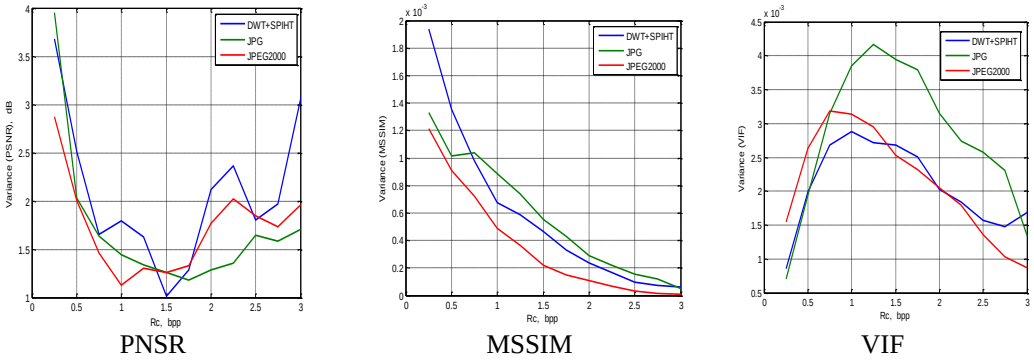

Figure 25. The variation of the variance of PSNR, MSSIM and VIF for the 20 selected satellite test images

6. CONCLUSION

In this research work, we proposed a selection algorithm of M images based on statistics calculated from images evaluation parameters (PSNR, MSSIM and VIF) according to choices of variances thresholds S_{PSNR}, S_{MSSIM} and S_{VIF}. We also applied the same algorithm of selection using three compression algorithms namely DWT+SPIHT, JPEG and JPEG2000. As perspective, we are going to apply the same algorithm of selection and compare the results including other methods of compression (wavelet-packet transform [17, 18] and quincunx transform [19-21]).

REFERENCES

[1] E. Sjöblom, *Compression of Medical Image Stacks using Wavelets and Zero Tree Coding", Master thesis, Division of Image Coding*, Department of Electrical Engineering, Linköping University junry, 2002.
[2] M.Beladgham et al., "Improving Quality of Medical Image Compression Using Biorthogonal CDF Wavelet Based on Lifting Scheme and SPIHT Coding", *serbian journal of electricatl engineering*, vol. 8(2), pp. 163-179, may 2011.
[3] M. Beladgham, *Construction d'une technique d'aide au diagnostic en imagerie médicale. Application a la compression d'images*, Doctoral thesis, University of Tlemcen, Dec 2012.
[4] T. Kavitha and K. Jayasankar, "Ideal Huffman Code for Lossless Image Compression for Ubiquitous Access," *IJEECS (Indonesian Journal of Electrical Engineering and Computer Science)*, vol. 12(2), Nov 2018.
[5] D. Taubman and M. Marcellin, *JPEG2000: Image compression fundamentals, standards and practice Boston*, Nov. 2001.
[6] Ph. Corvisier, "La Norme JPEG Adopte les Ondelettes," *Revue Electronique*, (9), pp. 15-165, Sep 1999.
[7] A. Trémeau, C. Fernandez-Maloigne & P. Bonton, *Image Numérique Couleur, de l'Acquisition au Traitemen*", Ed. DUNOD, 1984.
[8] C. Herley and M. Vetterli, "Wavelets and recursive filter banks," *IEEE Transaction on Signal Processing*, vol. 41(8), pp. 2536-2556, Aug 1993.
[9] CL. Guinet and J. Grellet, *Introduction à l'IRM De La Théorie A La Pratique*, Ed. Masson, 1992.
[10] M. Beladgham et al., "Medical Image Compression Using Quincunx Wavelets and SPIHT Coding," *Journal of Electrical Engineering & Technology*, vol. 7(2), pp. 264-272, 2012.

[11] H. R. Sheikh and A. C. Bovik, "Image Information and Visual Quality," *IEEE Transaction on Image Processing*, pp. 430-444, Sep 2004.
[12] E. Dumic, S. Grgic & M. Grgic, "New Image-Quality Measure Based on Wavelets," *Journal of Electronic Imaging*, vol. 19(1), pp. 011-018, Mar 2010.
[13] A. K. Moorthy, Z. Wang & A. C. Bovik, *Visual Perception and Quality Assessment*, Chapiter19 in Optical and digital image processing, Ed. Wiley, 2010.
[14] Z. Wang and Q. LI, "Information Content Weighting for Perceptual Image Quality Assessment," *IEEE Transactions on Image Processing*, vol. 20(5), pp. 1185-1198, May 2011.
[15] S. Dubuisson, D. Béréziat & N. Thome, *Bases du traitement des images - Opérations de Base et Améliorations*, 2016.
[16] N. T. Tankam., *Traitement Numérique d'Images et Applications : Méthodes statistiques optimisées pour le traitement numérique des images de grandes tailles*, Ed. Editions Universitaires Européènne, France, 2015.
[17] I. Benyahia, M. Beladgham & A. Bassou," Evaluation of the Medical Image Compression using Wavelet Packet Transform and SPIHT Coding", *IJECE (International Journal of Electrical and Computer Engineering)*, vol. 8(4), 2018.
[18] M. Latfaoui and F. Bereksi Reguig, "Packets Wavelets and Stockwell Transform Analysis of Femoral Doppler Ultrasound Signals," *IJECE (International Journal of Electrical and Computer Engineering)*, vol. 8(6), Dec 2018.
[19] F. Manuela, VD. Dimitri, U. Michael, "An Orthogonal Family of Quincunx Wavelets With Continuously Adjustable Order," *IEEE Transactions on Image Processing*, vol. 14(4), Apr 2005.
[20] V. D. Dimitri, B. Thierry & U. Michael, "On the Multidimensional Extension of the Quincunx Subsampling Matrix", *IEEE Signal Processing Letters*, vol. 12(2), Feb 2005.
[21] Y. Chen, A. D. Michael & L. Wu-Sheng, "Design of Optimal Quincunx Filter Banks for Image Coding," *EURASIP Journal on Advances in Signal Processing*, 2007.